AQUA
Water Infrastructure, Ecosystems and Society

Check for updates

IWA PUBLISHING

© 2023 The Authors AQUA — Water Infrastructure, Ecosystems and Society Vol 72 No 9, 1647 doi: 10.2166/aqua.2023.098

Ultrafiltration study of the polysulfone membrane modified with branched polyethyleneimine

Smit Vala[a], Sapna Ajay Gawali[a], Surendra Sasikumar Jampa[a], Manish Kumar Sinha[a,*] and Snigdha Khuntia[b]

[a] Department of Chemical Engineering, School of Technology, Pandit Deendayal Energy University, Gandhinagar 382 007, India
[b] School of Engineering and Applied Science, Ahmedabad University, Ahmedabad 380009, India
*Corresponding author. E-mail: manish.sinha@sot.pdpu.ac.in

MKS, 0000-0001-8076-0939

ABSTRACT

This work discussed the fabrication of polysulfone (PSF) ultrafiltration membranes with hydrophilic behaviour by adding branched polyethyleneimine (PEI) as an additive. By directly blending the base polymer and the additive in the organic solvent, the casting solution is prepared. An asymmetric ultrafiltration membrane was fabricated by the phase inversion method. The presence of PEI was confirmed by comparing the IR spectra of the plain PSF membrane and the modified PSF membrane. A scanning electron microscope was used for the comparison of morphological changes in plain and modified membranes. The membrane was characterised with respect to bovine serum albumin (BSA) adsorption, pure water flux, permeability, compaction factor, humic acid (HA) rejection, and water uptake. The fouling resistance behaviour is prompted due to the presence of hydrophilic PEI chains in the membrane. As a result, pure water flux and flux recovery ratio increased from 28.84 to 326.54 L/m^{2}h and from 0.526 to 0.954 L/m^{2}hkPa for the modified membrane with respect to the plain membrane, respectively.

Key words: fouling, hydrophilic, membrane, polysulfone

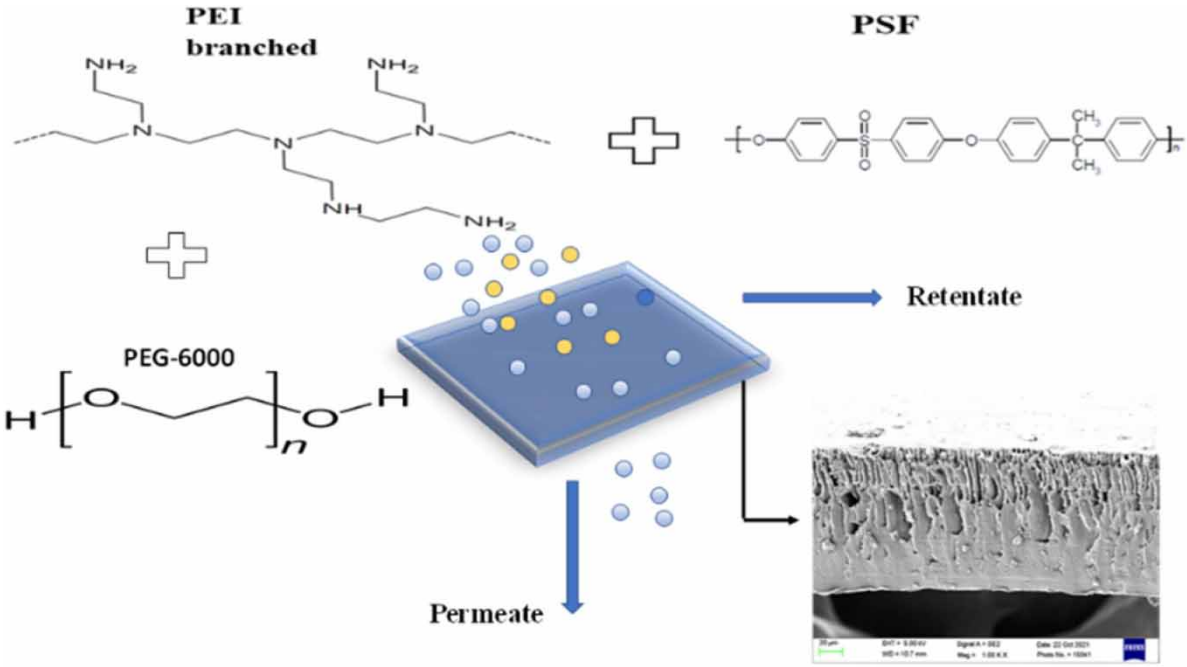
HIGHLIGHTS

- Polysulfone (PSF) ultrafiltration membranes with hydrophilic behaviour by adding the polyethyleneimine branched (PEI) as an additive were fabricated.
- High percentage of HA rejection was achieved with good antifouling properties.
- BSA adsorption also decreased with respect to the weight percentage of PEI.

This is an Open Access article distributed under the terms of the Creative Commons Attribution Licence (CC BY 4.0), which permits copying, adaptation and redistribution, provided the original work is properly cited (http://creativecommons.org/licenses/by/4.0/).

Downloaded from http://iwaponline.com/aqua/article-pdf/72/9/1647/1296349/jws0721647.pdf
by guest

GRAPHICAL ABSTRACT



NOMENCLATURE

A	effective membrane surface area (m^2)
A_s	membrane surface area (cm^2)
ATR-FTIR	Attenuated Total Reflectance-Fourier Transform Infrared
BSA	bovine serum albumin
C_a	BSA concentration after adsorption (mg/L)
CA	contact angle
C_b	BSA concentration before adsorption (mg/L)
C_f	feed concentration (mg/L)
CF	compaction factor
EWC	equilibrium water content
FESEM	field emission scanning electron microscope
Flux_{RR}	flux recovery ratio
F_t	total fouling ratio
F_{ir}	irreversible fouling ratio
F_r	reversible fouling ratio
HPG	hyperbranched polyglycerol
HA	humic acid
J_{w1}	pure water flux in first run (L/m^2 h)
J_{w2}	pure water flux in second run (L/m^2 h)
J_p	feed flux (L/m^2 h)
L	membrane thickness (cm)
LLDP	liquid–liquid displacement porosimetry
Ln	total hydraulic permeability coefficient
M_{BSA}	amount of BSA adsorbed (mg/cm^2)
M_{dry}	dry membrane weight (g)
M_{wet}	wet membrane weight (g)
NMP	*N*-methyl-2-pyrrolidone
o/w	oil-in-water
PEG	polyethylene glycol
PSF	polysulfone
PVDF	poly(vinylidene floride)

Downloaded from http://iwaponline.com/aqua/article-pdf/72/9/1647/1296349/jws0721647.pdf
by guest

PVP	polyvinylpyrrolidone
PWF	pure water flux
PEI	polyethyleneimine
R	rejection%
TMP	transmembrane pressure
UF	ultrafiltration
V	volume of permeate (L)
V_{BSA}	volume of BSA solution (L)
ΔP	operating pressure (kPa)
ΔT	permeation time (h)

Greek letters

σ	surface tension (mN/m)
ε	porosity
ρ_w	density of water (g/cm^3)

1. INTRODUCTION

Rapid societal growth leads to the expansion of industries, urban cities, and population growth, all of which increase the water demand and place enormous responsibility on the waste-water treatment process (Van Loosdrecht & Brdjanovic 2014). The volume of untreated wastewater discharged into the aquatic environment is currently increasing dramatically, and large quantities of hazardous chemicals that are non-biodegradable and highly toxic are contaminating freshwater bodies. Many polymers are used in waste-water treatment and the removal of toxic materials from water through the membrane separation process. The following are the advantages of membrane technology: (i) they are cost-effective, (ii) easy to operate, (iii) large temperature and pH operating range, and (iv) low energy consumption.

Polymeric materials have been thought to be an ideal candidate for membrane separation processes involving high process conditions. Most membranes are made of organic or inorganic materials. As a result, when compared to membranes made of other materials, polymer membranes are more effective. Polymers are the most important class of material for ultrafiltration membranes. The chemical and physical properties derived from structural components such as molecular weight, chain interaction, and chain flexibility are used to select the polymeric material for a specific membrane. The selection of a high-performance membrane material is critical. The materials used by researchers in the treatment of oily wastewater are as follows: polyvinylidene fluoride (PVDF) (Yuliwati & Ismail 2011; Zhang *et al.* 2013; Liu *et al.* 2016; Venault *et al.* 2016), polyethersulfone (PES) (Kusworo *et al.* 2017), polysulfone (PSF) (Sinha & Purkait 2013), polypropylone (PP) (Song *et al.* 2017), and cellulose acetate (Han *et al.* 2015) are all examples of base polymers. These polymeric materials are further modified by adding different types of additives depending on the requirement. Adding other materials can be achieved by various techniques based on polymer properties, solubility in different organic solvents, and weight percent of the additive requirement.

Polymer-based membranes with high pure water flux (PWF), rejection value, and hydrophilic properties are ideal for optimising oil/water separation performance. The need to deal with trade-off relationships between permeance and flux, as well as membrane fouling and membrane-scaling, is one of the critical issues pertaining to the use of conventional polymeric membranes in oily wastewater treatment (Zuo *et al.* 2018). Polymer-based membranes have low PWF, fouling issues, and degradation due to oil droplets blocking their pores, which causes the membranes to have short operation times.

Zhao *et al.* added hyperbranched polyglycerol (HPG) to a PVDF membrane as an additive. This experiment revealed that PVDF with HPG has higher PWF, porosity, and permeability than plain PVDF membranes (Zhao *et al.* 2007). Kim and Lee created a PSF polymer membrane with PEG 600 as an additive in 1998, and it was discovered that porosity and PWF were increased when compared to a plain PSF membrane (Kim & Lee 1998). Chakrabarty *et al.* investigated the effect of additive PEG with a mixture of different molecular weight poly(vinyl-pyrrolidone) (PVP) on the PSF (base polymer) membrane. The results were intriguing because the PWF of the modified membrane initially increased with the molecular weight of PVP up to 24,000 Da, but then the blended membrane began to become dense, resulting in decreases in PWF. Similarly, PEG with a molecular weight of 6,000 Da was found to have the highest BSA rejection. This experiment concluded that PEG with a molecular weight of 6,000 Da is the best additive or pore-forming agent for asymmetric PSF membranes (Chakrabarty *et al.* 2008). Saljioughi and Mohammadi investigated the effect of additive PVP blended in cellulose acetate at various weight percent

Downloaded from http://iwaponline.com/aqua/article-pdf/72/9/1647/1296349/jws0721647.pdf
by guest

levels ranging from 0 to 9 wt%. The findings showed conflicting results when using a 1.5 wt% additive. It was observed that the PWF of the membrane increased as the weight percent of PVP went from 0 to 1.5, due to the creation of macrovoids in the membrane's sublayer. However, increasing the weight percent of PVP above 1.5 resulted in a decrease in PWF, as macrovoid suppression occurred (Saljoughi & Mohammadi 2009).

Table 1 displays various hydrophilic polymers used in the literature as an additive for membrane modification. It is noted that this hydrophilic polymer used as an additive plays an important role in the mitigation of fouling tendency, and change in morphology and structure of polymeric membrane. Table 1 gives information about the base polymer used, different additives, organic solvent, PWF, and foulant rejection.

This research aims to evaluate the effectiveness of adding branched polyethyleneimine (PEI) to polysulfone (PSF) membranes for ultrafiltration to remove humic acid and oil–water emulsion. After that, the PSF membrane-modified with PEI was created and cast. Using Fourier Transform Infrared Attenuated Total Reflection Spectroscopy (FTIR-ATR) and Field Emission Scanning Electron Microscopy (FESEM), synthetic membranes were examined. PWF, HA rejection, BSA adsorption, permeability, and contact angle (CA) of membrane surface have been studied. The modified PSF membranes were found to have improved permeability, reduced fouling, and better selectivity compared to unmodified PSF membranes. The optimal PEI concentration for modifying the PSF membrane was determined to be 3 wt%, and the modified PSF membranes were effective in removing humic acid and oil–water emulsion from wastewater.

2. METHODS AND EXPERIMENTS

2.1. Materials

PSF (average $M_w = 35{,}000$ gmol) was used as the basic polymer in the membrane casting solution, which was purchased from Sigma-Aldrich Co., USA. N-methyl pyrrolidone (NMP) of analytical reagent-grade has been provided by LOBA Chemie, India. Sigma-Aldrich Co., USA and Otto Chemie Private Limited in India supplied bovine serum albumin (BSA). Without additional purification, all compounds were utilised. Throughout the studies, deionised (DI) water cleaned by the Millipore system (Millipore, France) was employed.

2.2. Synthesis and characterisation of membrane

PSF and PEI polymer were mixed in organic solvent NMP in which base polymer wt% was kept at 15 and 12% for two different sets. The PEG of molecular weight 6,000 Da was kept 5 wt% of the total weight of the solution, the combination was kept under constant heating at 45–50 °C under magnetic stirring. After cooling to room temperature, the solution was kept for degasification for 12–15 h and then the solution was fabricated with the help of a casting knife. The membrane was prepared by the phase inversion method by dipping the glass containing the solution into a DI water bath and was allowed to solidify and convert into a white colour sheet. The fabricated membranes were kept in replaced DI water bath for 12–15 h to remove unreacted polymer and eliminate the solvent remaining in the membrane.

Table 1 | Different polymer and additive used in literatures

Membrane polymer	Additive (Mol. wt)	Organic solvent	PWF (L/m^{2}h)	Foulant rejection	Reference
PSF (15 wt%)	PEG-600 to 12k Da	NMP	4.8×10^2	PEG (80%)	Kim & Lee (1998)
PSF (17.5 wt%)	PEG-600 Da	DMF	58.2	Protein (89%)	Arthanareeswaran *et al.* (2010)
Cellulose acetate	PVP 15,000 Da	NMP	64.5	–	Saljoughi & Mohammadi (2009)
PES	PEG-200, 400,600 Da	DMF	77	PEG (95%)	Idris *et al.* (2007)
PSF	PEG-400, 4,000, 10,000 Da	DMAc	4.2×10^3	BSA (75%) Pepsin (90%)	Ma *et al.* (2011)
PSF	PVP 10,000, 55,000 Da	DMAc	–	PVP (85%)	Matsuyama *et al.* (2003)
PSF	PEGME-550, 5,000 Da	NMP	4×10^2	BSA (85%)	Sinha & Purkait (2013)
PVDF	PEG 400 Da	TEP	1.7×10^3	Carbon ink (100%)	Zhang *et al.* (2017)
PVDF	PVA, PEG-1,000 Da	DMAc	5.5×10^2	BSA (92%)	Yuan & Ren (2017)
PVDF-co-HEP	mPEG-550, 5,000 Da	NMP	9.27×10^2	HA (99%), BSA (95%)	Singh & Purkait (2016)
PSF (12 wt%)	PEG-400, 6 K, 12K	NMP, DMAc	4.2×10^3	BSA (56.4%)	Chakrabarty *et al.* (2008)

Downloaded from http://iwaponline.com/aqua/article-pdf/72/9/1647/1296349/jws0721647.pdf
by guest

The presence of PEI and PSF of the produced membrane was confirmed by FTIR analysis. An FTIR spectrometer was used to get the FTIR spectra of the membrane, which was ground with KBr (IRAffinity-1, Shimadzu, Japan). The weight percentage of the additive is mentioned in Table 2.

2.3. Scanning Electron Microscope

FESEM (ZEISS LSM 510 Meta) was used to capture top surface and cross-sectional images of the PEI- branched PSF membranes. A sample of all membranes was mounted on a thin coating of a carbon tape on an FESEM stub of a suitable size. All of the samples were gold-coated to give electrical conductivity for non-conducting polymer membranes, and micrograph pictures were taken in an extreme vacuum with an acceleration voltage of 10–25 kV. At different magnifications, a number of SEM top and cross-section photos were captured. These photographs show the top layer's visual information as well as the membranes' cross-sectional structure.

2.4. ATR-FTIR study

The typical FTIR peaks of the PSF membrane were compared to the modified PSF membrane, indicating the presence of PEI in the membrane. The FTIR spectra of each modified membrane were obtained using a new attachment (ATR-8200 HA). The membrane samples were examined by attaching them to the ATR clamp.

2.5. Liquid–Liquid Displacement Porosimeter

Using the Liquid–Liquid Displacement Porosimeter (LLDP) method pore density, pore radius distribution, and mean pore radius of all membranes were measured. The LLDP method makes several assumptions, including that the membrane layer thickness is uniform throughout the surface, that the shape of the pores present in the membrane is cylindrical in nature for ease of calculation, that the pores are parallel to one another, not interconnected, and that the length of the pores is equal to the thickness of the skin layer. For an alcohol- and water-rich phase, a solution of methanol, iso-butanol, and water was used. The surface tension of the alcohol- and water-rich phases was 0.35 mN/m, and the dynamic viscosity of the water- and alcohol-rich phases was 3.4 mNs/m^2. For an alcohol- and water-rich phase, a solution of methanol, iso-butanol, and water was used. The surface tension of the alcohol- and water-rich phases was 0.35 mN/m, and the dynamic viscosity of the water- and alcohol-rich phases was 3.4 mNs/m^2. The correlation data of the radius of pores were calculated using Equation (1) (also known as Cantor's equation) (r).

$$r = \frac{2\sigma}{P} \tag{1}$$

where P denotes transmembrane pressure (TMP) and σ denotes the difference in surface tension between the water and alcohol phases. Equation (2) was used to calculate the pore counts per unit membrane surface area ($N_{i,k}$).

$$N_{i,k} = \frac{d\eta}{2\pi\sigma^4} P_{i,k}^3 J_{i,k} \tag{2}$$

Pore counts per unit surface area with a radius between r_i and r_k are represented by $N_{i,k}$. The dynamic viscosity of the alcohol-rich phase is denoted by d, which is the pore length as well as the thickness of the membrane layer.

Table 2 | Weight percent of membrane solution

Membrane name	Base polymer PSF (WT%)	Additive PEI (wt%)	Pore-forming agent PEG (wt%)	Solvent NMP (wt%)
15M0	15.00	0	5	80
15M1	15.00	1	5	79
12M2	12.00	2	5	81
12M3	12.00	3	5	80

Downloaded from http://iwaponline.com/aqua/article-pdf/72/9/1647/1296349/jws0721647.pdf
by guest

Equation (3) was used to calculate the total number of pores (N_t) per unit area of the membrane: As a result, the mean pore radius (r_m) was calculated using the following formula (Equation (4)).

$$N_t = \Sigma N_{i,k} \tag{3}$$

$$r_m = \frac{\Sigma N_{i,k}\, r_{i,k}}{\Sigma N_{i,k}} \tag{4}$$

2.6. Porosity measurement

Gravimetric methods were used to evaluate the membrane porosity (ε). A membrane of size 8 cm^2 was cut first, then immersed in DI water for 4 h before being reweighted. In this example, the membrane porosity can be calculated using Equation (5).

$$\epsilon = \frac{\omega_1 - \omega_2}{A \times L \times dW} \tag{5}$$

Here, ω_1 and ω_2 are the weights of the membrane after and before soaking, respectively. L is the thickness of the membrane obtained from SEM. A is the effective area of membrane soaked in water, while dW is the water density (1 gm/cm^3).

2.7. Permeation study of casted membranes

The experiments were carried out in a 1-l stainless steel membrane cell, using flat circular membranes with a diameter of 0.052 m. Therefore, a membrane with an effective area of 0.00221 m^2 was utilised. For 1 h, PWF was calculated at a TMP of 2.5 kg/cm^2. The water permeation flux measured at 30-min intervals is used to calculate the compaction factor (CF). The CF is the ratio of initial PWF to the steady state PWF. The set-up used for PWF, permeability, and CF evaluation is shown in Figure 1. The PWF was calculated using the following equation

$$J_w = \frac{Q}{A \times \Delta t} \tag{6}$$

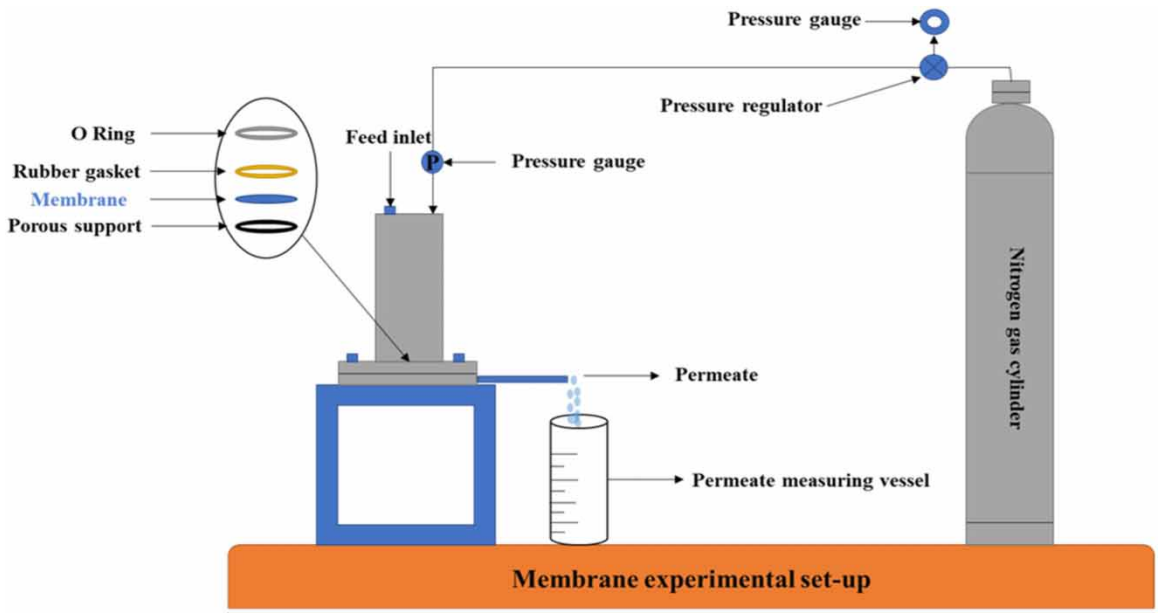


Figure 1 | Experimental set-up for the permeation study.

Downloaded from http://iwaponline.com/aqua/article-pdf/72/9/1647/1296349/jws0721647.pdf
by guest

2.8. Wastewater preparation and analysis

The ultrafiltration process was tested with three distinct types of contaminants: (i) humic acid, (ii) oil/water emulsion, and (iii) BSA protein solution at concentrations of 100, 100, and 1,000 ppm, respectively. The concentrations of HA, o/w emulsion, and BSA were plotted against matching absorbance values of wavelengths using a UV-VIS spectrophotometer (Model: DR 6000, Hach). The calibration curves for HA and o/w emulsion are shown in Figures 2 and 3.

2.9. Fouling study

BSA adsorption and HA rejection tests were utilised to explore the rejection of protein (solute), organic compounds, and water flux values of the modified membranes. While keeping the concentration constant at 1,000 mgL^{-1}, the protein (BSA) was disintegrated in DI water. Similarly, 100 mgL^{-1} of HA was kept as the concentration for each experiment. In the experiment, pure water flux (J_{w1}) for 1 h was observed then the feed was changed to HA solution and the experiment

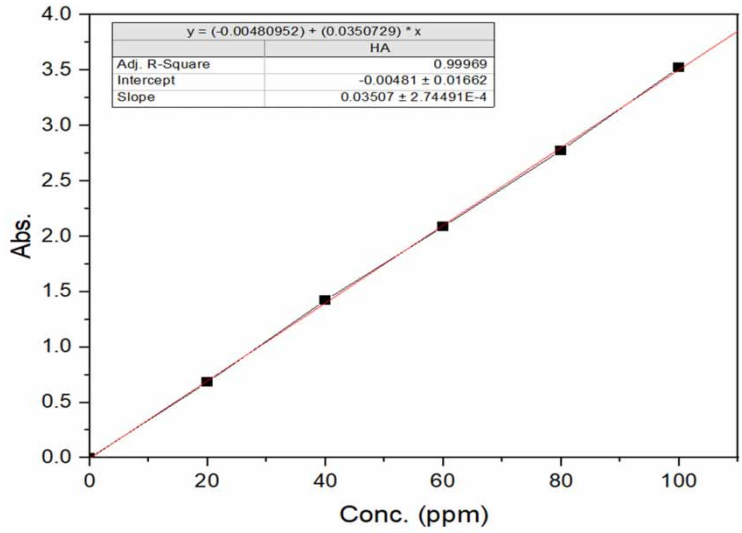


Figure 2 | HA calibration curve.

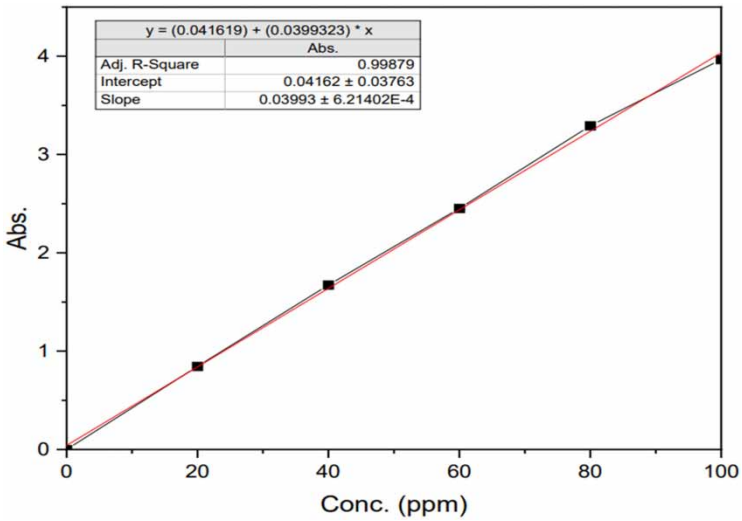


Figure 3 | Oil–water emulsion calibration curve.

Downloaded from http://iwaponline.com/aqua/article-pdf/72/9/1647/1296349/jws0721647.pdf
by guest

was continued for HA flux (J_p) for 1 h, after calculating HA flux, the membrane was washed with DI water and pure water flux (J_{w2}) was measured again for 1 h. For the BSA adsorption study the pieces of membranes were dipped into BSA solution in different solution holders and kept for 1 day and the concentrations of the resulting solutions were calculated using a UV-visible spectrophotometer. The accompanying Equations (7) and (8) were utilised to figure out the rejection percentage and BSA adsorption.

$$R\ (\%) = \left[1 - \left(\frac{C_p}{C_f}\right)\right] \times 100 \tag{7}$$

$$C_{ad} = \frac{(C_b - C_a)\ V_{BSA}}{A_s} \tag{8}$$

where C_p and C_f are concentration permeate and feed, respectively. R is the rejection ratio in percentage. V_{BSA} is the volume of BSA used for adsorption C_b, C_a are values of concentration of BSA solution before and after the adsorption, respectively.

The flux recovery ratio (Flux-RR) was evaluated using J_{w1} and J_{w2}. Flux loss is caused by membrane fouling (J_{w1}–J_p). There are some ratios to characterise the fouling process that can be used to study the antifouling property (Wang *et al.* 2005). F_t is the degree of total flux loss caused by total fouling, and it is the first ratio. Other ratios include F_r and F_{ir}. Reversible fouling is F_r, and irreversible fouling is F_{ir}. Membrane surface fouling results from reversible fouling, which can be removed with water cleaning. F_{ir}, on the other hand, is produced by irreversible protein adsorption into membrane pores and cannot be removed by simple backwashing. The equation used for calculating F_t, F_r, F_{ir} and Flux-RR is as follows:

$$F_t = \frac{(1 - J_p)}{J_{w1}} \tag{9}$$

$$F_r = \frac{(J_{w2} - J_p)}{J_{w1}} \tag{10}$$

$$F_{ir} = \frac{(J_{w1} - J_{w2})}{J_{w1}} \tag{11}$$

$$Flux - RR = \frac{J_{w2}}{J_{w1}} \times 100 \tag{12}$$

3. RESULTS AND CHARACTERISATION

3.1. ATR-FTIR AND FESEM

As shown in Figure 4, The presence of the amide group was confirmed by 1,476 cm^{-1} peak, and another peak at 2,950 cm^{-1} get broader with an increase in wt% of the copolymer due to the –C–H– stretching, while the peaks at 1,155 and 1,295 cm^{-1} are typical of polysulfone polymer. These findings suggest that PEI was thoroughly mixed in the PSF membrane. Figure 5 shows SEM images of the 15M0 and 12M3 PSF membranes' top surfaces figure a and b show SEM images of the 15M0 and 12M3 PSF membranes cross section surface SEM images are shown in figure c and d. In comparison to the controlled PSF membrane, the top surface of the modified membranes has a significantly rougher surface. The surface of blended membranes got increasingly rough as the weight percent of PEI rose. This roughness was caused by polymer settlement on the membrane surface. The number of these structures and porosity grew as the wt% of PEI in the modified membranes increased. The cross-section images show finger-like pore structure in the 15M0 membrane while for 12M3 the cross section image has more vigorous pore structure due to the mixing of PEI branched in the PSF membrane. This roughness is caused by polymer settlement on the membrane surface.

3.2. Liquid–Liquid Displacement Porosimetry study

The liquid–liquid displacement Porosimetry (LLDP) is a method used to perform an in-line porosimetry analysis of the membrane cartridges, getting their pore size distributions (PSDs), and mean pore diameters (d_{avg}). This will enable us to get the pore size and pore density of each pore in the membrane. Here, a mixture of water, isobutanol, and methanol in a ratio of 25:15:7 v/v was used in surface tension between alcohol- and water-rich phases. A mixture of water and alcohol was

Downloaded from http://iwaponline.com/aqua/article-pdf/72/9/1647/1296349/jws0721647.pdf
by guest

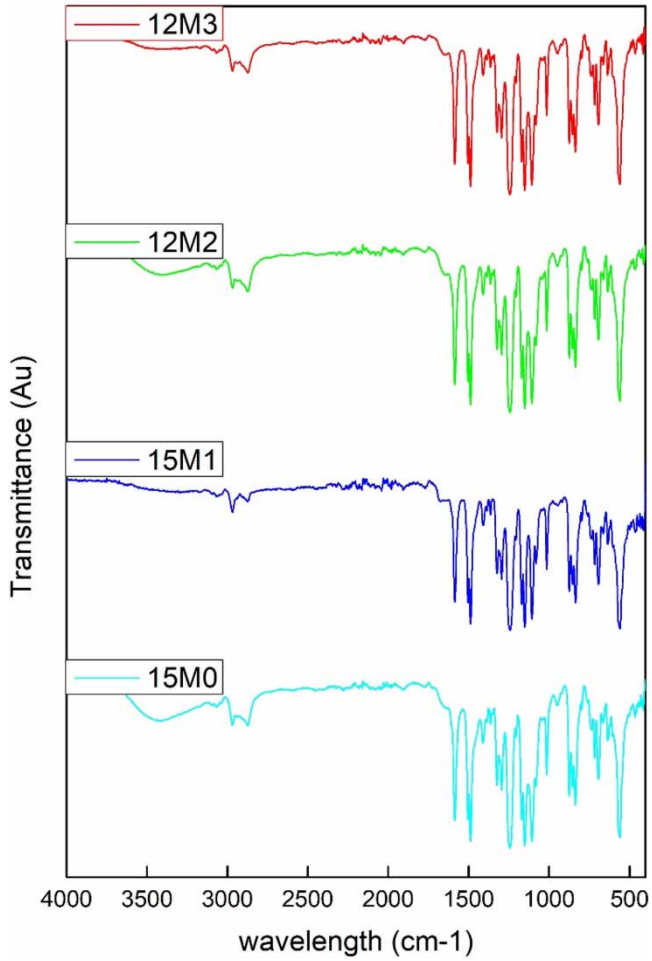


Figure 4 | Fourier Transform Infrared Attenuated Total Reflection Spectroscopy of PEI/PSF membranes.

shaken in a separating funnel and was left to stand for 4 h to ensure complete separation between the two liquids. The water-rich phase settled at the bottom of the funnel and the alcohol-rich phase remained at the top. The bottom product was used as a wetting liquid for the membrane and the top product for displacing liquids as discussed in the section "Methods and experiments".

Figure 6 shows the relationship between flux and pressure for PEI/PSF membranes. Initially, 40 kPa was set at the beginning of the experiment. As the pressure was increased the flux increased with a rapid rise between 200 and 400 kPa. As the flux increased the pore size also grew larger. It can be observed from the graph that 15M0 and 15M1 had the same rate throughout and 12M3 had a higher rate than all. From Figure 7, we can see that the pore density was high for 2 nm particle size for all the membranes and after 4 nm the pore density was zero. Figure 8 shows the pore distribution across the membrane as we can see that the graph is almost similar for all the membranes which mean that the membranes have the same pore distribution size but after 4 nm the pore size tends to nil. Figure 9 represents the cumulative pore number (%) with different pore sizes. For 3–18 nm, the cumulative pore size was 100% making it suitable for ultrafiltration.

3.3. Pure water flux, CF, water CA, and hydraulic permeability

The CA is a simple approach to determine a membrane's relative hydrophilicity/hydrophobicity. Hydraulic permeability, IEC capacity, CF, and CA for 15M0, 15M1, 12M2, and 12M3 membranes are shown in Table 3. CA reduces as the weight percent of copolymer increases as shown in Figure 10 from 55° for plain PSF membrane to 44° for 2 wt% modified PEI/PSF membrane. PEI blended PSF membranes are more hydrophilic due to the membrane's structure, particularly the membrane

Downloaded from http://iwaponline.com/aqua/article-pdf/72/9/1647/1296349/jws0721647.pdf
by guest

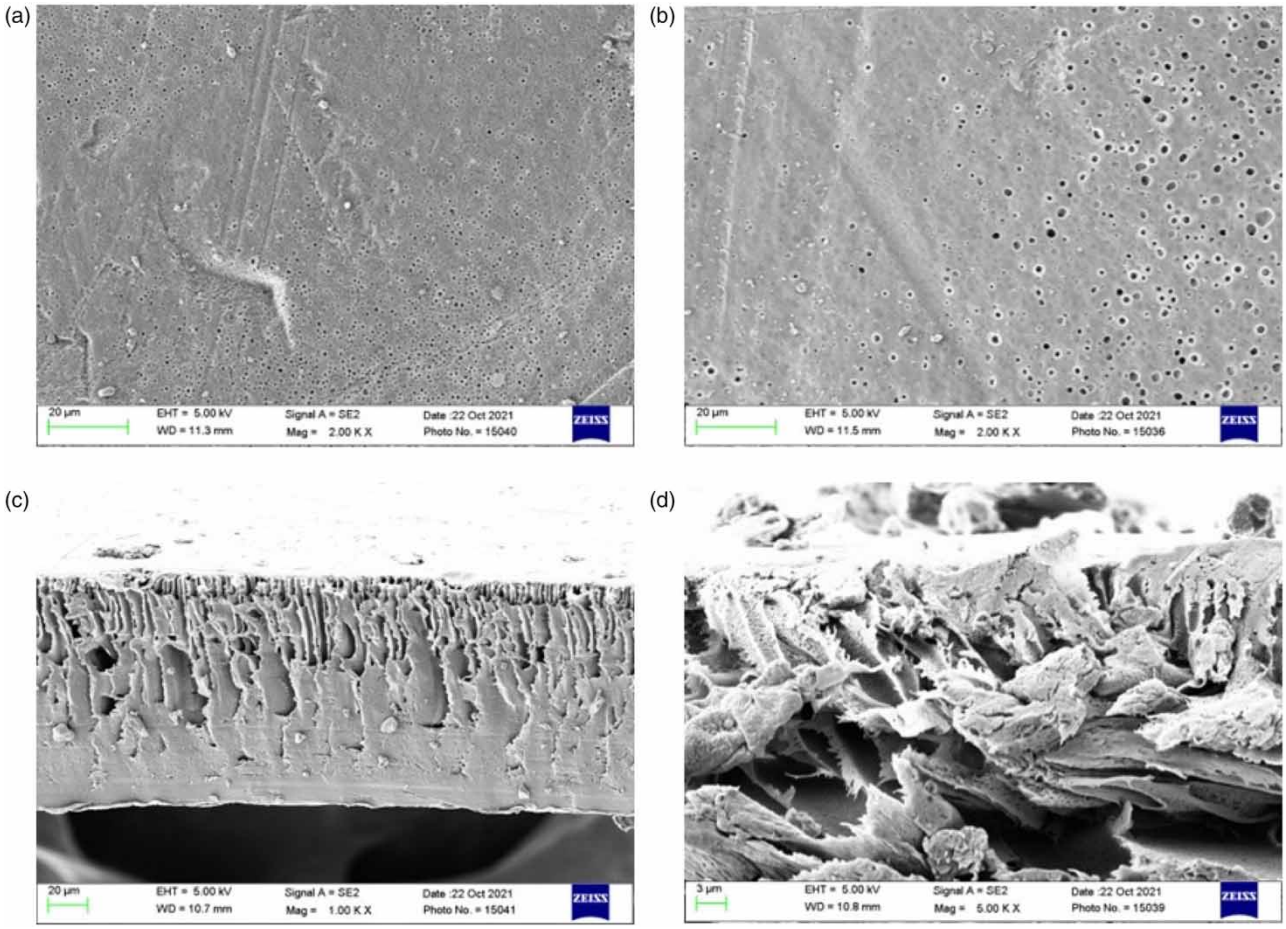


Figure 5 | FESEM images: (a) top view of 15M0, (b) top view of 12M3, (c) cross-section view of 15M0 and (d) cross-section view of 12M3.

sublayer which is referred to as the CF. The presence of many macro voids in the sublayer causes the membrane to compact. The higher the CF, the more probable the membrane compacts. Figure 11 shows the PWF for all membranes. PWF decreased substantially with time because of compaction for all membranes, reaching a stable state at roughly 60 min. The steady state PWF increases as the weight percent of PEI increases, as shown in Figure 12.

3.4. Ultrafiltration study

Wastewater was subjected to testing using a batch filtration cell in order to assess membrane permeability in both HA removal and flux filtration. During ultrafiltration, a solution containing 100 ppm of humic acid was utilised for every pre-compacted membrane. This experiment needed a time span of 3 h. Therefore the timing started at 0 and continued until it reached 60 min. After measuring the PWF and giving it the label (J_{w1}), the HA flux was measured from 60 to 120 min and given the label (J_p). After that, the membrane was cleaned with plain water, and PWF was measured again from 120 to 180 min. data identified as (J_{w2}), we can determine the HA flux, the Flux-RR, the total flow, the irreversible flux, and the reversible flux. The same steps must be used when separating oily wastewater. Figure 12 and Figure 13 represent the time-dependent flux of humic acid and the o/w emulsion ultrafiltration; the fouling study of humic acid and the o/w emulsion ultrafiltration examination are shown in Figures 14 and 15, respectively. Pure water flux (PWF) decreased somewhat in the first few minutes of pure water permeation in studies including o/w emulsion ultrafiltration and humic acid. Still, it remained constant for all membranes after 40 min (Figures 12 and 13). The J_{w2} values of the modified membranes were lower than the J_{w1} values (0–60 min), but higher than the J_p values. The modified membranes excelled over the plain membranes (15M0) in all ultrafiltration examinations. As shown in Figure 14, flux loss in HA permeation was reduced

Downloaded from http://iwaponline.com/aqua/article-pdf/72/9/1647/1296349/jws0721647.pdf
by guest

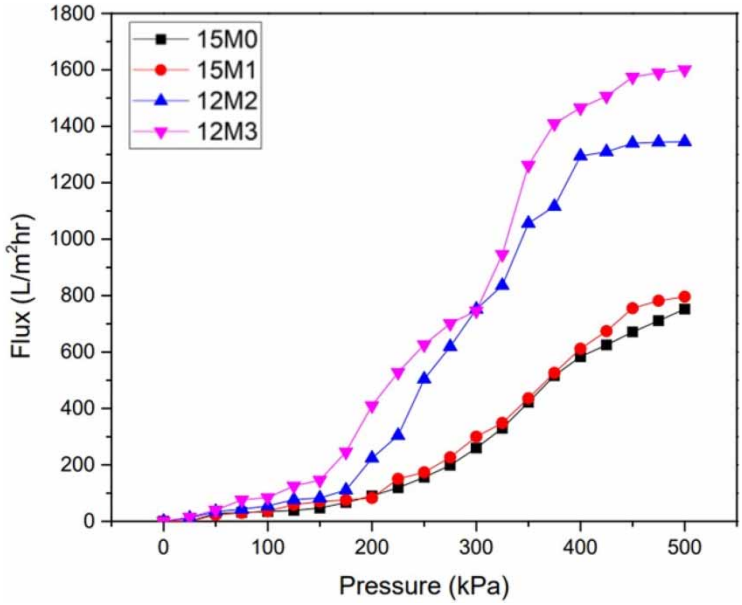


Figure 6 | Flux vs. pressure for LLDP studies of plain and modified membranes.

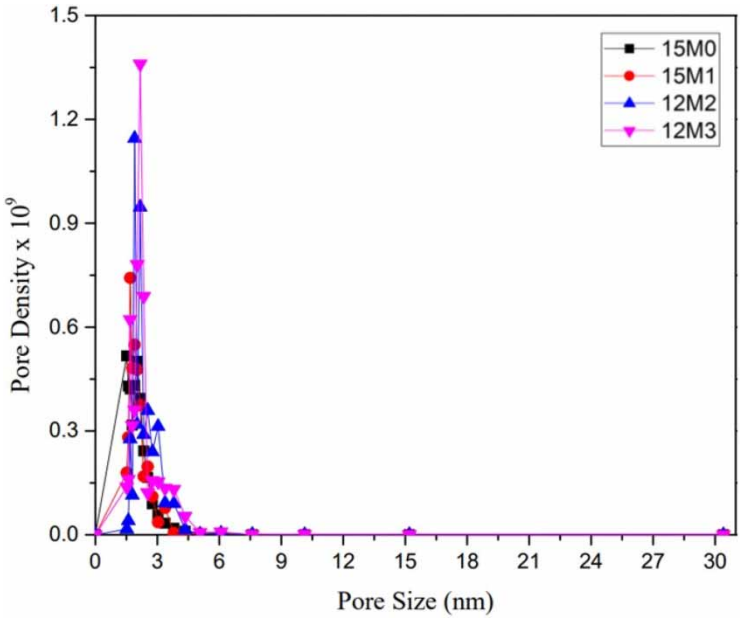


Figure 7 | Pore density vs. pore size of plain and modified membranes.

throughout the humic acid ultrafiltration process, with less flux loss due to humic acid. This happens because the membrane on the surface makes it simple to maintain the cross-linked HA molecules in place. HA molecules create a cross-linked mesh gel layer with one another. Since the gel layer around the HA molecules is porous and mesh-like, there would be negligible flux loss. Moreover, in the instance of an oil/water emulsion, the flow of oil/water emulsion decreased throughout the 30 min of ultrafiltration because oil droplets were absorbed by the pores and blocked them. After around 30 min, oil droplets began to adsorb and accumulate on the membrane's surfaces, making it stable.

Downloaded from http://iwaponline.com/aqua/article-pdf/72/9/1647/1296349/jws0721647.pdf
by guest

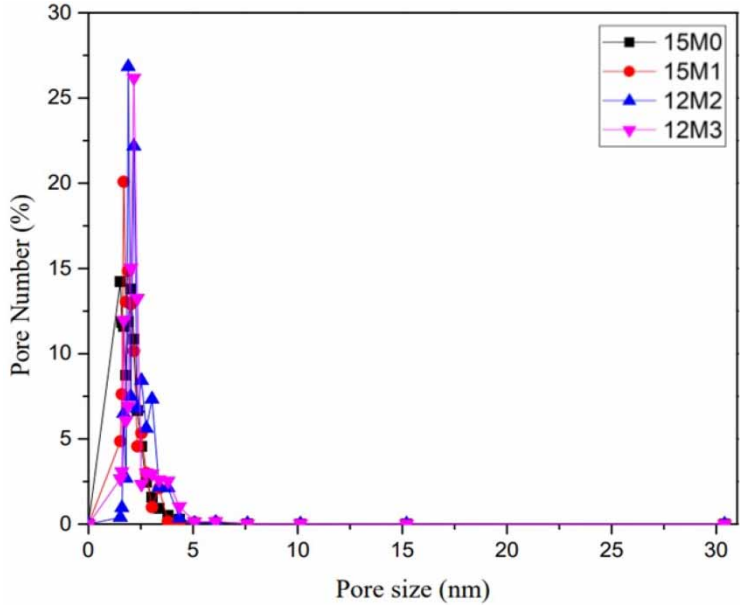


Figure 8 | Pore number (%) vs. pore size of plain and modified membranes.

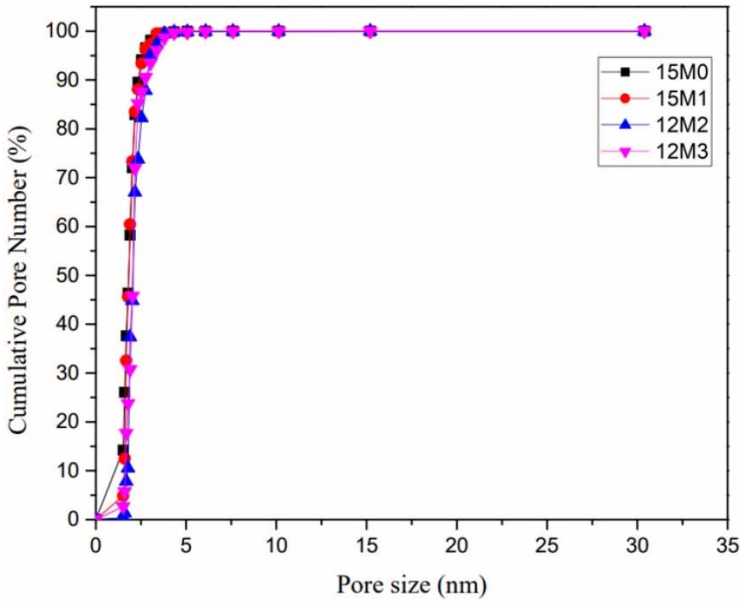


Figure 9 | Cumulative pore number (%) vs. pore size of plain and modified membranes.

Table 3 | Pure water flux (PWF), compaction factor (CF), and permeability of plain and modified membranes

Membrane	PWF (L/m^{2}h)	CF	Permeability (L/m^{2}h Kpa)
15M0	28.84	1.37	0.19
15M1	48.97	1.66	0.27
12M2	299.3121	1.45	0.57
12M3	326.5319	2.5	0.78

Downloaded from http://iwaponline.com/aqua/article-pdf/72/9/1647/1296349/jws0721647.pdf
by guest

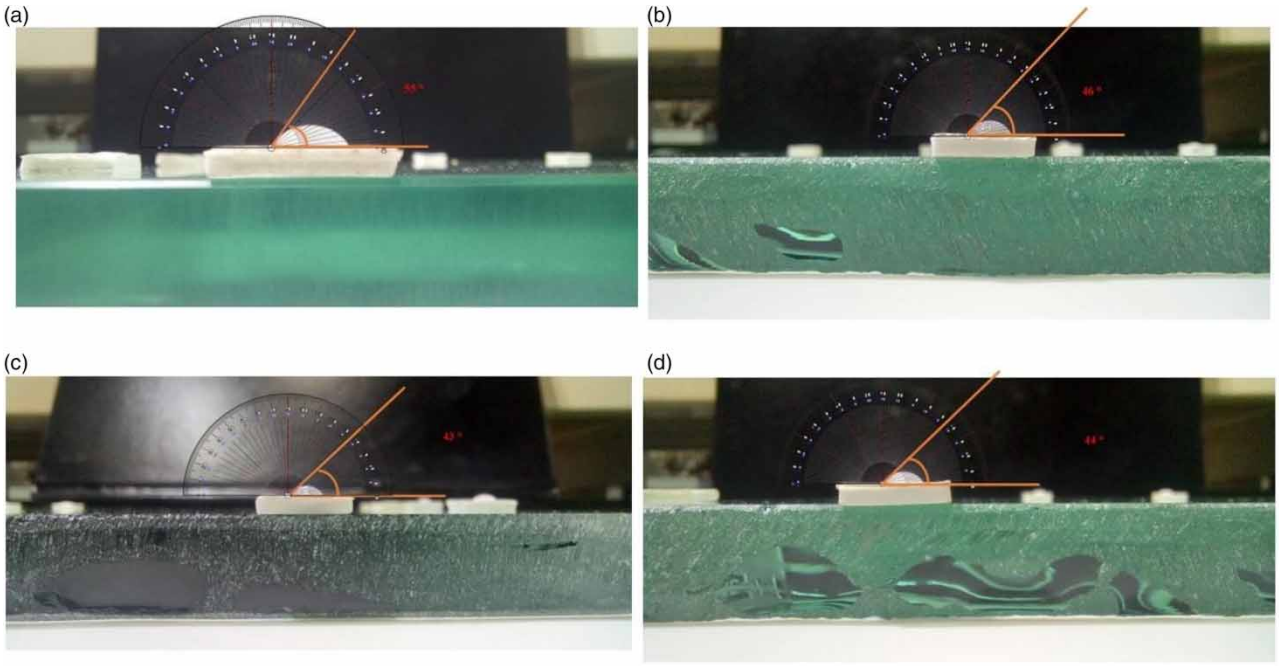


Figure 10 | Water CA: (a) 15M0, (b) 15M1, (c) 12M2, and (d) 12M3 (PEI/PSF).

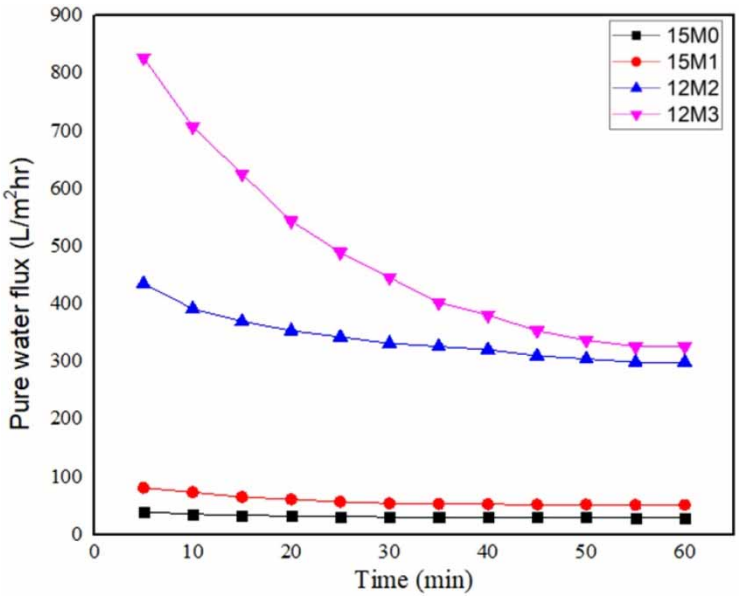


Figure 11 | Time-dependent pure water flux.

F_r, F_t, and F_{ir} ratios were examined and are provided to understand how humic acid ultrafiltration causes membrane fouling fully. Tables 4 provides more data. As shown in Figures 14 and 15, irreversible fouling was reduced after initially rising in the instance of 15M0 when PEI was present at a concentration of 3 wt%. Less foulant build-up or deposition in the membrane's pores or on its surface is indicated by lower F_{ir} levels, and vice versa. The concentration of PEI may increase reversible fouling by up to 3 wt%. The rise in F_r demonstrated that reversible fouling of the membrane takes the place of irreversible fouling

Downloaded from http://iwaponline.com/aqua/article-pdf/72/9/1647/1296349/jws0721647.pdf
by guest

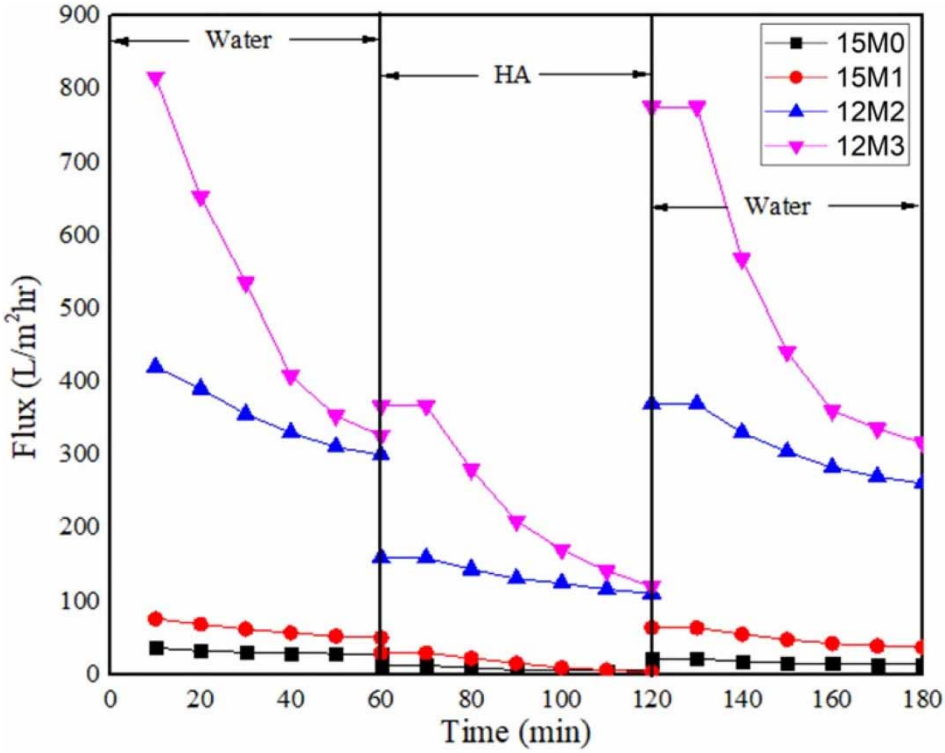


Figure 12 | Time-dependent flux for fouling study using HA.

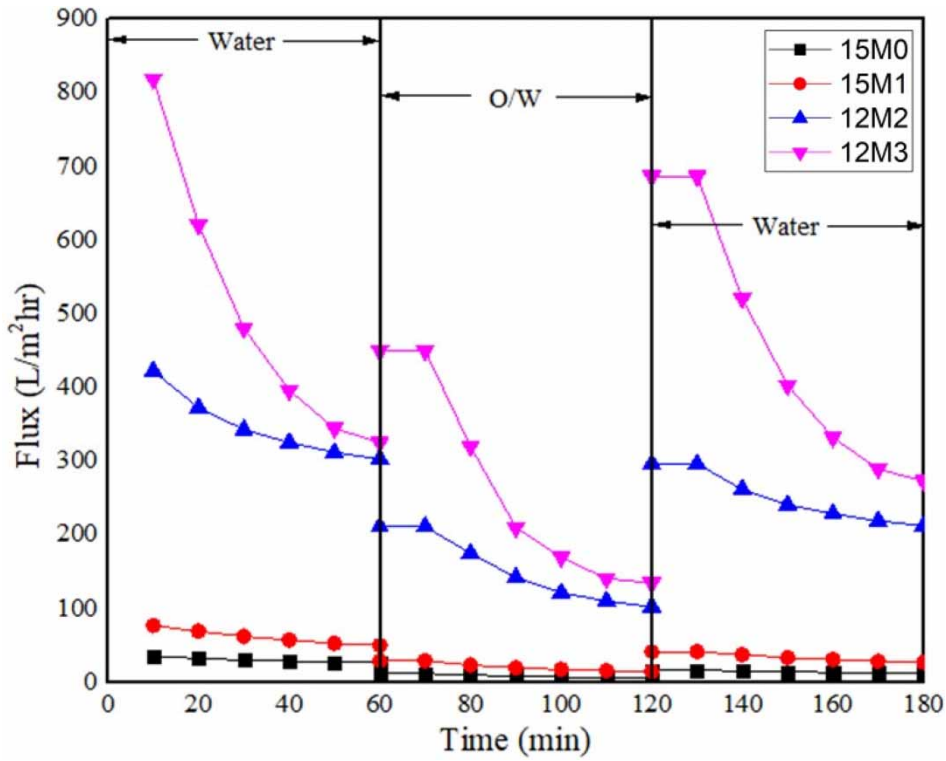


Figure 13 | Time-dependent flux for fouling study using oil–water emulsion.

Downloaded from http://iwaponline.com/aqua/article-pdf/72/9/1647/1296349/jws0721647.pdf
by guest

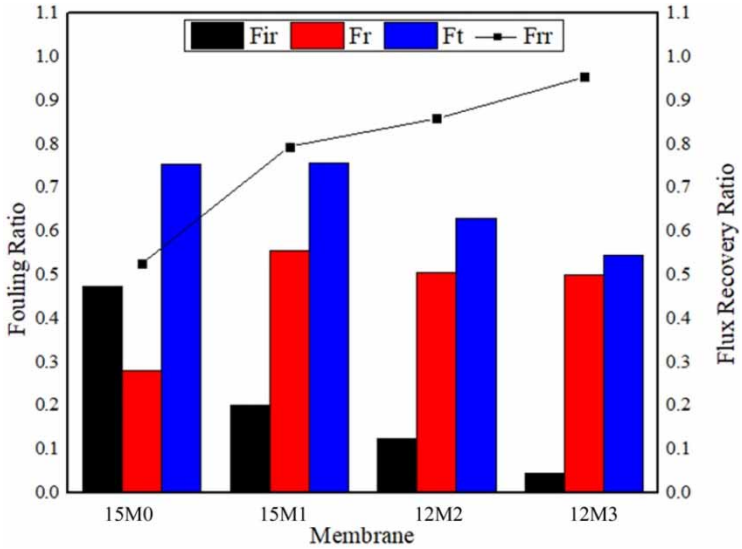


Figure 14 | Fouling ratio and flux recovery ratio while using HA.

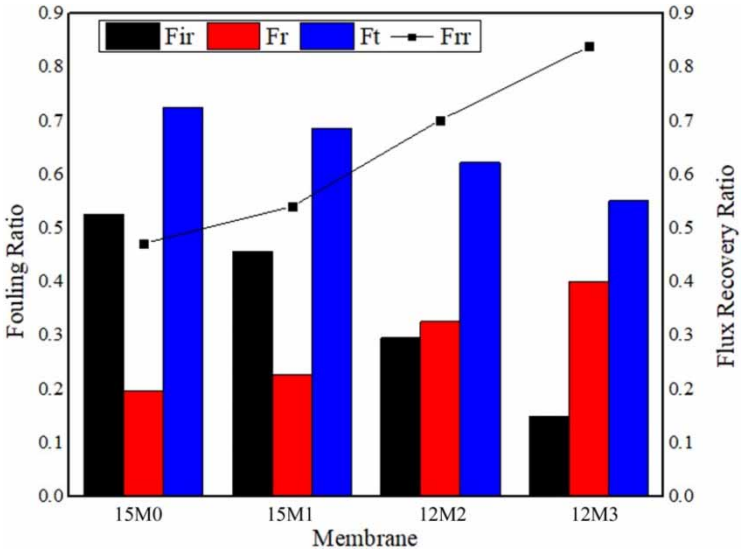


Figure 15 | Fouling ratio and flux recovery ratio while using oil–water emulsion.

during the ultrafiltration process. In other words, incorporating PEI on the membrane surface prevents irreversible fouling. The detail explains these findings that the hydration layer generated on the membrane surface can reduce the contact between the foulants and the surface of the membrane by the incorporation of the amine group, preventing the irreversible foulant binding. Similar to F_{ir}, the trend in F_t was seen. It was determined from Figures 14 and 15 that in ultrafiltration studies with all types of feeds (HA and o/w emulsion), the bare membrane has the maximum value of F_t and F_{ir}. However, the 15M3 membrane has the least value of F_t and F_{ir}, making it less responsive to the deposition of irreversible foulants. The Flux_{RR} of unmodified and modified membranes is shown in Figures 14 and 15. Flux_{RR} improves for modified membranes as F_{ir} decreases because Flux_{RR} and irreversible fouling are directly related to each other. The Flux_{RR} enhanced from 0.526 (for plain PSF membrane) to 0.954, and 0.85 (for 12M3 membrane) in the humic acid and oil–water emulsion ultrafiltration process, respectively. Compared to HA ultrafiltration, the value of Flux_{RR} in oil–water emulsion ultrafiltration was

Downloaded from http://iwaponline.com/aqua/article-pdf/72/9/1647/1296349/jws0721647.pdf
by guest

Table 4 | Comparison of reported PEI-based polysulfone membrane with present study for foulant rejection

Sr. NO	POLYMER	ADDITIVES	REMARK	APPLICATION	REFERENCES
1	PES	PEI	PWF = 359.0 L/m^2 h, Rejection OF (BSA) bovine serum albumin = 96.1%, at PEI loading = 3 wt%	BSA removal	Fang *et al.* (2015)
2	PS	PEI	Water Permeability = 22.66 L/hm^2 bar, Rejection rate of acid orange(AO-74) = 68.5% and methyl orange(OM) = 64.7%, at PEI loading = 20 wt%	soluble azoic dyes removal	Benkhaya *et al.* (2020)
3	PSF	PEI/ $CaCO_3$	PWF = 145 L/m^2 h, Rejection OF (BSA) bovine serum albumin = 92% and oil rejection = 90%, at PEI loading = 2 wt% and $CaCO_3$ loading = 10 wt%	BSA and oil removal	Saki & Uzal (2018)
4	PSF	PEI	PWF = 326.54 L/m^2 h, Rejection OF (HA) Humic Acid = 61.08%, at PEI loading = 3 wt%	Humic Acid removal	This work

lower. This might be because HA molecules are easily removed by simply hydraulic cleaning and require higher $Flux_{RR}$. Due to the oil–water emulsion's insolubility in water, oil droplets persist within the pores or on the membrane surface even after simple hydraulic washing, making it challenging to clean the membranes. Therefore, chemical cleaning can eliminate these types of foulants from membranes.

4. CONCLUSION

PEI used as an additive in PSF base polymer membrane has shown positive results such as the decrease in fouling ratio and increase in the rejection value of HA along with the increase in the weight percentage of PEI in composition from 0 to 3%. The permeability of the membrane 12M3 has increased from 0.19 to 0.78 L/m^{2}hr Kpa with respect to the membrane 15M0. The rejection value of HA increased from 9.32 to 61.088% for 0–3% of PEI. Overall, the difficulty in the direct blending of PEI with PSF is a major issue due to the agglomeration of PEI particles on the membrane surface. For a higher weight percentage of PEI in PSF base polymer membrane, the co-polymerisation process can be utilised for better fouling ratio results and rejection percentage.

DATA AVAILABILITY STATEMENT

All relevant data are included in the paper or its Supplementary Information.

CONFLICT OF INTEREST

The authors declare there is no conflict.

REFERENCES

Arthanareeswaran, G., Mohan, D. & Raajenthiren, M. 2010 Preparation, characterization and performance studies of ultrafiltration membranes with polymeric additive. *Journal of Membrane Science* **350** (1–2), 130–138. doi:10.1016/j.memsci.2009.12.020.

Benkhaya, S., M'rabet, S., Hsissou, R. & El Harfi, A. 2020 Synthesis of new low-cost organic ultrafiltration membrane made from Polysulfone/Polyetherimide blends and its application for soluble azoic dyes removal. *Journal of Materials Research and Technology* **9** (3), 4763–4772. doi:10.1016/j.jmrt.2020.02.102.

Chakrabarty, B., Ghoshal, A. K. & Purkait, M. K. 2008 Preparation, characterization and performance studies of polysulfone membranes using PVP as an additive. *Journal of Membrane Science* **315** (1–2), 36–47. doi:10.1016/j.memsci.2008.02.027.

Fang, X., Li, J., Li, X., Sun, X., Shen, J., Han, W. & Wang, L. 2015 Polyethyleneimine, an effective additive for polyethersulfone ultrafiltration membrane with enhanced permeability and selectivity. *Journal of Membrane Science* **476**, 216–223. doi:10.1016/j.memsci.2014.11.021.

Han, G., de Wit, J. S. & Chung, T. S. 2015 Water reclamation from emulsified oily wastewater via effective forward osmosis hollow fiber membranes under the PRO mode. *Water Research* **81**, 54–63. doi:10.1016/j.watres.2015.05.048.

Idris, A., Mat Zain, N. & Noordin, M. Y. 2007 Synthesis, characterization and performance of asymmetric polyethersulfone (PES) ultrafiltration membranes with polyethylene glycol of different molecular weights as additives. *Desalination* **207** (1–3), 324–339. doi:10.1016/j.desal.2006.08.008.

Kim, J. H. & Lee, K. H. 1998 Effect of PEG additive on membrane formation by phase inversion. *Journal of Membrane Science* **138** (2), 153–163. doi:10.1016/S0376-7388(97)00224-X.

Downloaded from http://iwaponline.com/aqua/article-pdf/72/9/1647/1296349/jws0721647.pdf
by guest

Kusworo, T. D., Qudratun & Utomo, D. P. 2017 Performance evaluation of double stage process using nano hybrid PES/SiO2-PES membrane and PES/ZnO-PES membranes for oily waste water treatment to clean water. *Journal of Environmental Chemical Engineering* **5** (6), 6077–6086. doi:10.1016/j.jece.2017.11.044.

Liu, D., Zhu, J., Qiu, M. & He, C. 2016 Antifouling performance of poly(lysine methacrylamide)-grafted PVDF microfiltration membrane for solute separation. *Separation and Purification Technology* **171**, 1–10. doi:10.1016/j.seppur.2016.07.006.

Ma, Y., Shi, F., Ma, J., Wu, M., Zhang, J. & Gao, C. 2011 Effect of PEG additive on the morphology and performance of polysulfone ultrafiltration membranes. *Desalination* **272** (1–3), 51–58. doi:10.1016/j.desal.2010.12.054.

Matsuyama, H., Maki, T., Teramoto, M. & Kobayashi, K. 2003 Effect of PVP additive on porous polysulfone membrane formation by immersion precipitation method. *Separation Science and Technology* **38** (14), 3449–3458. doi:10.1081/SS-120023408.

Saki, S. & Uzal, N. 2018 Preparation and characterization of PSF/PEI/CaCO3 nanocomposite membranes for oil/water separation. *Environmental Science and Pollution Research* **25** (25), 25315–25326. doi:10.1007/s11356-018-2615-9.

Saljoughi, E. & Mohammadi, T. 2009 Cellulose acetate (CA)/polyvinylpyrrolidone (PVP) blend asymmetric membranes: preparation, morphology and performance. *Desalination* **249** (2), 850–854. doi:10.1016/j.desal.2008.12.066.

Singh, R. & Purkait, M. K. 2016 Evaluation of mPEG effect on the hydrophilicity and antifouling nature of the PVDF-co-HFP flat sheet polymeric membranes for humic acid removal. *Journal of Water Process Engineering* **14**, 9–18. doi:10.1016/j.jwpe.2016.10.001.

Sinha, M. K. & Purkait, M. K. 2013 Increase in hydrophilicity of polysulfone membrane using polyethylene glycol methyl ether. *Journal of Membrane Science* **437**, 7–16. doi:10.1016/j.memsci.2013.03.003.

Song, Y. Z., Kong, X., Yin, X., Zhang, Y., Sun, C-C., Yuan, J-J., Zhu, B. & Zhu, L-P. 2017 Tannin-inspired superhydrophilic and underwater superoleophobic polypropylene membrane for effective oil/water emulsions separation. *Colloids and Surfaces A: Physicochemical and Engineering Aspects* **522**, 585–592. doi:10.1016/j.colsurfa.2017.03.023.

Van Loosdrecht, M. C. M. & Brdjanovic, D. 2014 Anticipating the next century of wastewater treatment. *Science* **344** (6191), 1452–1453. doi:10.1126/science.1255183.

Venault, A., Wei, T-C., Shih, H-S., Yeh, C-C., Chinnathambi, A., Alharbi, S. A., Carretier, S., Aimar, P., Lai, J-Y. & Chang, Y. 2016 Antifouling pseudo-zwitterionic poly(vinylidene fluoride) membranes with efficient mixed-charge surface grafting via glow dielectric barrier discharge plasma-induced copolymerization. *Journal of Membrane Science* **516**, 13–25. doi:10.1016/j.memsci.2016.05.044.

Wang, Y. Q., Wang, T., Su, Y., Peng, F., Wu, H. & Jiang, Z. 2005 Remarkable reduction of irreversible fouling and improvement of the permeation properties of poly(ether sulfone) ultrafiltration membranes by blending with pluronic F127. *Langmuir* **21** (25), 11856–11862. doi:10.1021/la052052d.

Yuan, H. & Ren, J. 2017 Preparation of poly(vinylidene fluoride) (PVDF)/acetalyzed poly(vinyl alcohol) ultrafiltration membrane with the enhanced hydrophilicity and the anti-fouling property. *Chemical Engineering Research and Design* **121**, 348–359. doi:10.1016/j.cherd.2017.03.023.

Yuliwati, E. & Ismail, A. F. 2011 Effect of additives concentration on the surface properties and performance of PVDF ultrafiltration membranes for refinery produced wastewater treatment. *Desalination* **273** (1), 226–234. doi:10.1016/j.desal.2010.11.023.

Zhang, S., Wang, R., Zhang, S., Li, G. & Zhang, Y. 2013 Development of phosphorylated silica nanotubes (PSNTs)/polyvinylidene fluoride (PVDF) composite membranes for wastewater treatment. *Chemical Engineering Journal* **230**, 260–271. doi:10.1016/j.cej.2013.06.098.

Zhang, H., Lu, X., Liu, Z., Zhong, M., Wu, S., Li, Z., Kong, X & Wu, C. 2017 Study of the dual role mechanism of water-soluble additive in low temperature thermally-induced phase separation. *Journal of Membrane Science* **543** (May), 1–9. doi:10.1016/j.memsci.2017.08.032.

Zhao, Y. H., Zhu, B-K., Ma, X-T, & Xu, Y-T. 2007 Porous membranes modified by hyperbranched polymers. I. Preparation and characterization of PVDF membrane using hyperbranched polyglycerol as additive. *Journal of Membrane Science* **290** (1–2), 222–229. doi:10.1016/j.memsci.2006.12.037.

Zuo, J. H, Cheng, P., Chen, X-F., Yan, X., Guo, Y-J. & Lang, W-Z. 2018 Ultrahigh flux of polydopamine-coated PVDF membranes quenched in air via thermally induced phase separation for oil/water emulsion separation. *Separation and Purification Technology*. doi:10.1016/j.seppur.2017.10.027.

First received 28 June 2022; accepted in revised form 5 August 2023. Available online 17 August 2023

Downloaded from http://iwaponline.com/aqua/article-pdf/72/9/1647/1296349/jws0721647.pdf
by guest